Research Square

Preprints are preliminary reports that have not undergone peer review. They should not be considered conclusive, used to inform clinical practice, or referenced by the media as validated information.

A Framework for Time-Explicit Life Cycle Optimization

Timo Diepers
RWTH Aachen University https://orcid.org/0009-0002-8566-8618
Jan Tautorus
Interdisciplinary Transformation University Austria https://orcid.org/0009-0002-9216-870X
Jan Marcus Hartmann
RWTH Aachen University https://orcid.org/0000-0002-4295-1299
Niklas von der Assen
niklas.vonderassen@ltt.rwth-aachen.de

RWTH Aachen University https://orcid.org/0000-0001-8855-9420

Research Article

Keywords: temporal distribution, temporal evolution, transformation pathways, dynamic, prospective life cycle assessment, industrial decarbonization

Posted Date: May 8th, 2026

DOI: https://doi.org/10.21203/rs.3.rs-9630408/v1

License: This work is licensed under a Creative Commons Attribution 4.0 International License.
Read Full License

Additional Declarations: The authors declare no competing interests.

A Framework for Time-Explicit Life Cycle Optimization

Timo Diepers[a], Jan Tautorus[b], Jan Hartmann[a], and Niklas von der Assen[a]

[a] *Institute of Technical Thermodynamics, RWTH Aachen University, Germany*

[b] *Interdisciplinary Transformation University, Austria*

Abstract

Life cycle optimization (LCO) selects optimal processes and supply chains from a set of alternatives given environmental constraints and objectives, supporting the design of sustainable systems and their transitions. However, current approaches rely on static assumptions, overlooking two interacting temporal dimensions: *temporal distribution* (flows are spread over time) and *temporal evolution* (processes and supply chains change over time). Because distribution dictates flow timing and evolution dictates flow magnitude, both must be considered jointly to accurately assess cumulative environmental impacts and time-specific environmental constraints. We present a framework for time-explicit LCO that captures these interdependencies to determine optimal transition pathways. The framework tracks flow timing relative to process installation and dynamically determines flow magnitudes from vintage-dependent process parameters and time-specific background supply chains. A case study on integrated methanol and pig iron production demonstrates how time-explicit LCO enables optimization against time-resolved environmental impacts and constraints, revealing mitigation strategies inaccessible to static approaches: prioritizing early high-efficiency technology installation to idle older processes

as operational savings outweigh embodied impacts of stranded assets, and avoiding transient resource bottlenecks through diversification. To facilitate widespread application, we provide the open-source Python package `optimex`, enabling practitioners to design transition pathways that rigorously respect environmental limits.

Graphical Abstract

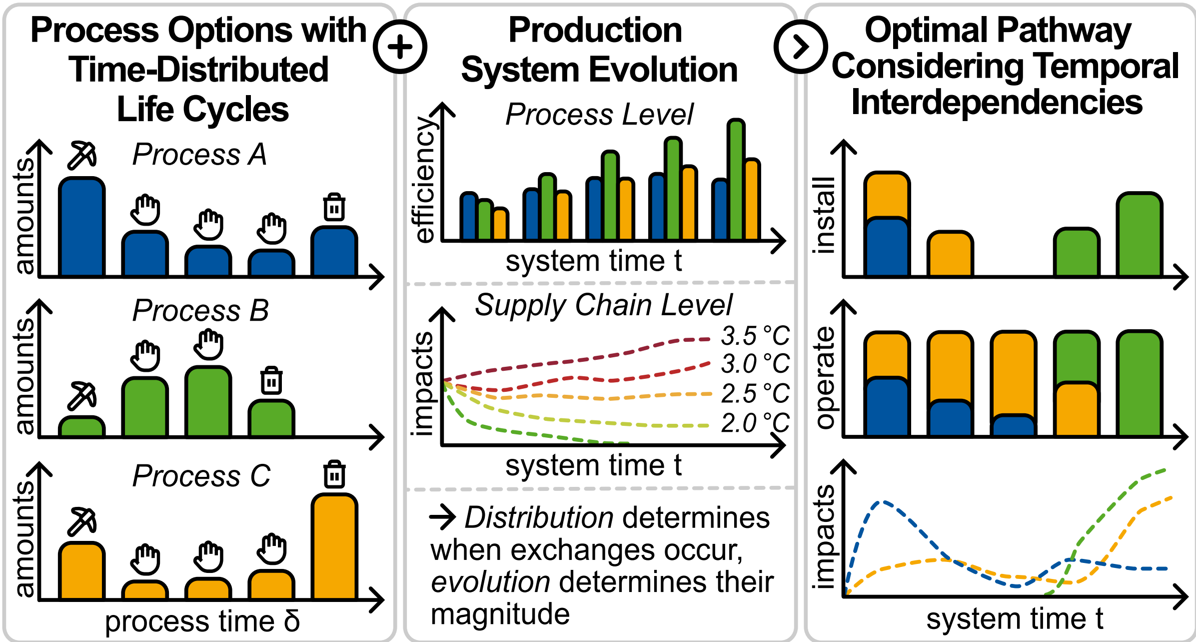

Keywords: temporal distribution, temporal evolution, transformation pathways, dynamic, prospective life cycle assessment, industrial decarbonization

1 Introduction

Anthropogenic systems must transition towards environmental sustainability[1,2]. Environmental sustainability encompasses two fundamental sets of constraints: stock-related limits, such as finite mineral resources[3] and cumulative carbon budgets[4,5], and flow-related limits, dictating maximum rates at which resources can be extracted or emissions assimilated by the biosphere[3,6]. Any viable transition pathway needs to rigorously respect both sets of constraints.

While Integrated Assessment Models (IAMs) are primary instruments for navigating these transitions, their simplified representations of specific technologies prevent them from identifying the specific bottlenecks within technologies' supply chains or emission profiles that violate stock- and flow-related environmental limits[7–9]. Sector- or process-specific optimization models improve on the technological resolution, yet they often neglect upstream supply chains or environmental impact categories besides climate change, risking environmental burden shifting[10,11].

To holistically consider a broad range of environmental impact categories across entire supply chains, researchers increasingly couple sector- or process-specific optimization models with Life Cycle Assessment (LCA) in Life Cycle Optimization (LCO)[11–17]. However, current LCO approaches typically rely on a static representation of life cycle impacts, assuming all intermediate flows (i.e., exchanges within the production system) and elementary flows (i.e., exchanges between production system and environment) occur simultaneously. This assumption neglects the temporal interdependencies between two fundamental temporal dimensions: *temporal distribution* and *temporal evolution*[18]. First, real-world life cycles can span multiple years or decades, leading to time lags between different processes and their intermediate and elementary flows (*temporal distribution*)[19–22]. Second, processes and supply chains change over time, leading to differing intermediate and elementary flow profiles at different points in time (*temporal evolution*)[23–25]. By neglecting both dimensions, current LCO approaches risk designing pathways that violate environmental constraints when deployed in practice.

For transition pathways, these two temporal dimensions are inextricably linked. *Distribution* determines when a flow occurs, while *evolution* determines the magnitude of a flow at that specific time. Consequently, both dimensions jointly dictate whether a transition pathway stays within (1) stock-related limits, because distribution and evolution together alter the total cumulative impact over the transition period, where the impact at one point in time depends on the previous stock level, and (2) flow-related limits, because the combination of distribution and evolution can shift the timing and scale of a flow's peak. Optimization models therefore need to account for these temporal interdependencies to ensure environmentally sustainable pathways.

While the *assessment* of transition pathways under consideration of temporal distribution and evolution is enabled by time-explicit LCA[18], its integration into optimization models for the *design* of transition pathways remains incomplete. Current attempts mainly address temporal evolution: Reinert et al.[26] and Charalambous et al.[27] couple energy system models with time-specific background supply chains, and Thakker and Bakshi[28] optimize a transition of the chemical industry incorporating learning curves and ongoing decarbonization. Similarly, Hung et al.[29] consider the temporal evolution of the electricity sector, alongside stock dynamics. However, these contributions disregard the temporal distribution of life cycles, assuming all flows occur at the moment of a technology's installation. This assumption creates a structural inability to model the interaction between system-specific time lags and supply chain shifts. For example, ignoring the decades-long lag between a facility's construction and its end-of-life means the model cannot account for newly available treatment processes at the actual time of decommissioning, which were not available at the time of installation. Consequently, models that solely focus on temporal evolution risk violating stock- and flow-related environmental limits. As two recent reviews conclude, full time-differentiation remains a significant gap in LCO[30,31].

In this work, we propose a framework for time-explicit LCO of transition pathways.

By simultaneously considering the temporal distribution and evolution of process's intermediate and elementary flows, our framework identifies pathways that rigorously respect both stock- and flow-related environmental constraints. To achieve this, our framework tracks the timing of flows relative to a process's installation, and dynamically determines the magnitues of flows at that specific time from vintage-dependent process parameters and time-specific background supply chains. To facilitate the widespread adoption of time-explicit LCO, we provide an implementation of the framework in the open-source Python package `optimex`, which integrates with the `Brightway` LCA framework[32] and the `pyomo` optimization framework[33]. The application of time-explicit LCO is demonstrated in a case study on the transition of an integrated industrial system co-producing methanol and pig iron.

2 Time-Explicit Life Cycle Optimization Framework

As the basis for time-explicit LCO, we first review the mathematical formulation of static LCO in Section 2.1. Building on this, we then introduce a mathematical framework for time-explicit LCO in Section 2.2, extending static LCO to simultaneously consider temporal distribution and evolution of processes' intermediate and elementary flows. Next, in Section 2.3, we outline the operationalization of the proposed framework, detailing how the mathematical framework can be integrated in common LCA and LCO modeling practices. Finally, Section 2.4 briefly introduces a Python-based implementation of the framework in the `optimex` package.

2.1 Foundation

In matrix-based LCA, environmental impacts $\boldsymbol{h}$ are calculated by characterizing a life cycle inventory $\boldsymbol{g}$ using a characterization matrix $\boldsymbol{Q}$:

$$\boldsymbol{h} = \boldsymbol{Q}\,\boldsymbol{g} \tag{1}$$

The life cycle inventory $\boldsymbol{g}$ is determined from the biosphere matrix $\boldsymbol{B}$ and the scaling vector $\boldsymbol{s}$:

$$\boldsymbol{g} = \boldsymbol{B}\,\boldsymbol{s} \tag{2}$$

In turn, $\boldsymbol{s}$ is determined from the technosphere matrix $\boldsymbol{A}$ and the functional unit or demand vector $\boldsymbol{f}$:

$$\boldsymbol{s} = \boldsymbol{A}^{-1}\,\boldsymbol{f} \tag{3}$$

In LCO, the technosphere matrix $\boldsymbol{A}$ is not square, as multiple processes (i.e., columns) can produce the same products (i.e., rows). As a result, the system has degrees of freedom: different combinations of process scaling factors can satisfy the same product demand. These degrees of freedom can be exploited through optimization. Since only a square $\boldsymbol{A}$ is invertible, $\boldsymbol{s}$ cannot be determined directly from Eq. 3 in LCO. Instead, the scaling vector $\boldsymbol{s}$ is made the decision variable of an optimization problem, where $\boldsymbol{s}$ is determined such that the demand $\boldsymbol{f}$ is satisfied while minimizing or maximizing an objective function. A linear LCO problem with the objective to minimize environmental impact h^{c}, where c is a specific chosen impact category, can be formulated as:

$$\min_{\boldsymbol{s}} \quad h^{\mathrm{c}} = \boldsymbol{Q}^{\mathrm{c}}\,\boldsymbol{g} = \boldsymbol{Q}^{\mathrm{c}}\,\boldsymbol{B}\,\boldsymbol{s} \tag{4a}$$

$$\text{s.t.} \quad \boldsymbol{A}\,\boldsymbol{s} = \boldsymbol{f}, \tag{4b}$$

$$\boldsymbol{s} \geq \boldsymbol{0}. \tag{4c}$$

2.2 Formulation

In the static LCO formulation described in Eq. 4, neither temporal distribution nor temporal evolution of intermediate and elementary flows can be considered. In this Section, we extend static to time-explicit LCO in four steps by (1) introducing explicit temporal dimensions and reflecting time lags through convolution, (2) enabling temporal evolution through vintage-dependent parameters, (3) differentiating installation- and operation-dependent flows, and (4) incorporating time-specific background systems. Finally, we compose the fully time-explicit LCO problem.

2.2.1 Time-Explicit Matrices and Convolution

To make the static LCO formulation (Eq. 4) time-explicit, we add temporal dimensions to its matrices and vectors. We introduce system time $t \in \mathcal{T}$, representing absolute points in time (e.g., January 1, 2026). Several quantities from the static formulation naturally extend to system time: the demand vector $\boldsymbol{f}_t$ specifies required product amounts at each point in time, the scaling vector $\boldsymbol{s}_t$ represents process scaling decisions at each point in time, and the characterization matrix $\boldsymbol{Q}_t^{\mathrm{c}}$ allows for time-specific characterization factors.

The technosphere and biosphere matrices $\boldsymbol{A}$ and $\boldsymbol{B}$, however, cannot simply be indexed by system time t. Their coefficients describe intermediate and elementary flows that are distributed across a process's life cycle. This temporal profile is intrinsic to each process: Regardless of when a process is installed, the relative timing of its flows remains the same. Since the installation time is itself a decision variable in LCO, these profiles cannot be expressed in absolute time. We therefore introduce process time $\delta \in \mathit{\Delta}$, representing time relative to the installation of a process. The matrices $\boldsymbol{A}_\delta$ and $\boldsymbol{B}_\delta$ define what share of each flow occurs at what time delta relative to a process's installation at $\delta = 0$. For example, a process installed at $t = 2025$ can have its end-of-life treatment defined at $\delta = 10$ years, translating to absolute time $t = 2035$.

With $\boldsymbol{A}_\delta$ and $\boldsymbol{B}_\delta$ defined in process time and $\boldsymbol{s}_t$ in system time, we need a mechanism to bridge the two temporal dimensions. Convolution achieves this by summing, for each system time t, over all processes whose life cycle overlaps with t:

$$(\boldsymbol{A} * \boldsymbol{s})_t = \sum_{\delta \in \mathit{\Delta}_t} \boldsymbol{A}_\delta \, \boldsymbol{s}_{t-\delta}, \tag{5a}$$

$$(\boldsymbol{B} * \boldsymbol{s})_t = \sum_{\delta \in \mathit{\Delta}_t} \boldsymbol{B}_\delta \, \boldsymbol{s}_{t-\delta}. \tag{5b}$$

where $\mathit{\Delta}_t = \{\delta \in \mathit{\Delta} \mid t - \delta \in \mathcal{T}\}$ is the subset of valid process time deltas at system time

t. The convolution yields the time-explicit inventory $\boldsymbol{g}_t$, which captures all elementary flows occurring at each absolute point in time:

$$\boldsymbol{g}_t = (\boldsymbol{B} * \boldsymbol{s})_t \tag{6}$$

Analogously, the demand satisfaction constraint ensures that intermediate flows balance at each point in time:

$$(\boldsymbol{A} * \boldsymbol{s})_t = \boldsymbol{f}_t \tag{7}$$

The total environmental impact in a specific category h^{c} is then obtained by summing the characterized inventory over all time steps:

$$h^{\mathrm{c}} = \sum_{t \in \mathcal{T}} \boldsymbol{Q}_t^{\mathrm{c}} \boldsymbol{g}_t \tag{8}$$

This formulation captures temporal distribution, i.e., the time lags between a process's installation and its subsequent flows. However, $\boldsymbol{A}_\delta$ and $\boldsymbol{B}_\delta$ as defined here do not yet reflect temporal evolution: the coefficients are the same regardless of when a process is installed.

2.2.2 Temporal Evolution through Vintage-Dependent Parameters

To capture temporal evolution, we note that the process-specific matrix coefficients of $\boldsymbol{A}$ and $\boldsymbol{B}$ are locked in at the moment of installation and do not change afterward. Simply indexing $\boldsymbol{A}$ and $\boldsymbol{B}$ by system time t would therefore not reflect this lock-in. We instead introduce the vintage $v \in \mathcal{T}$, representing the installation time of each process unit. The individual coefficients of $\boldsymbol{A}$ and $\boldsymbol{B}$ become $a_{p,i,\delta,v}$ and $b_{p,e,\delta,v}$, respectively, where p denotes the process, i the intermediate flow, and e the elementary flow. Each coefficient thus depends on both process time δ and vintage v, such that a process installed at vintage v has its flows distributed according to δ and its flow magnitudes determined by v. The convolution from Eq. 5 generalizes to:

$$(\boldsymbol{A} * \boldsymbol{s})_t = \sum_{v \in \mathcal{V}_t} \boldsymbol{A}_{\delta=t-v,\,v}\, \boldsymbol{s}_v, \tag{9a}$$

$$(\boldsymbol{B} * \boldsymbol{s})_t = \sum_{v \in \mathcal{V}_t} \boldsymbol{B}_{\delta=t-v,\,v}\, \boldsymbol{s}_v. \tag{9b}$$

Here, $\mathcal{V}_t = \{v \in \mathcal{T} \mid t - v \in \Delta\}$ is the set of vintages with flows occurring at system time t, determined by whether the process time $\delta = t - v$ falls within the defined time deltas Δ. For example, a process installed at $v = 2025$ evaluated at $t = 2030$ has $\delta = 5$, meaning it is five years into its life cycle. The coefficient $a_{p,i,\delta,v}$ thus captures both the life cycle stage (via $\delta = t - v$) and installation time (via v).

To express technology evolution, we apply multiplicative scaling factors $\phi_{p,i,v}$ to base coefficients:

$$a_{p,i,\delta,v} = \phi_{p,i,v} \cdot a^{\text{base}}_{p,i,\delta}, \quad b_{p,e,\delta,v} = \phi_{p,e,v} \cdot b^{\text{base}}_{p,e,\delta} \tag{10}$$

where $a^{\text{base}}_{p,i,\delta}$ and $b^{\text{base}}_{p,e,\delta}$ are the base (vintage-independent) coefficients. A scaling factor $\phi_{p,i,v} = 0.7$ indicates a 30% improvement relative to the base amount of the respective flow.

2.2.3 Differentiating Installation- and Operation-Dependent Flows

So far, the scaling vector $\boldsymbol{s}$ scales all flows of a process jointly: installing one unit of capacity triggers both construction-related and operation-related flows in fixed proportion. In traditional LCA and LCO, this coupling is unavoidable because all flows are temporally aggregated. Because our formulation explicitly resolves time, we can distinguish between flows tied to the installation of a process (e.g., construction materials, end-of-life treatment) and flows tied to its operation (e.g., fuel consumption, operational emissions). This allows operational flows to scale independently of installed capacity: a gas power plant's fuel use can vary over time without affecting its construction footprint; in other words, a constructed power plant does not always need to operate at full capacity. To reflect this differentiation, we split the scaling vector into two components: capacity installation $\boldsymbol{s}_v$ (indexed by vintage v) and operational level $\boldsymbol{o}_{t,v}$ (indexed by system time t and vintage v).

To distinguish operation and installation on the flow-level, we collect all operation-dependent intermediate and elementary flows in a set $\mathcal{O}$ and define separate matrices for operation ($\boldsymbol{A}_v^{\mathrm{op}}$, $\boldsymbol{B}_v^{\mathrm{op}}$) and capacity installation ($\boldsymbol{A}_{\delta,v}^{\mathrm{cap}}$, $\boldsymbol{B}_{\delta,v}^{\mathrm{cap}}$). The operation matrices $\boldsymbol{A}_v^{\mathrm{op}}$ and $\boldsymbol{B}_v^{\mathrm{op}}$ contain per-unit-operation coefficients for flows in $\mathcal{O}$, with vintage-specific values reflecting technology evolution (Eq. 10). The capacity matrices $\boldsymbol{A}_{\delta,v}^{\mathrm{cap}}$ and $\boldsymbol{B}_{\delta,v}^{\mathrm{cap}}$ contain all flows not in $\mathcal{O}$, with the rest of the coefficients set to zero.

The inventory $\boldsymbol{g}_t^{\mathrm{flex}}$ now combines contributions from both capacity and operation matrices. Capacity-related flows (construction, end-of-life) can occur for any vintage v whose life cycle overlaps with t, captured by $\mathcal{V}_t$ as before. Operational flows, however, can only occur while a process is still running. We restrict them to vintages within their operational lifetime by defining $\mathcal{V}_t^{\mathrm{op}} = \{v \in \mathcal{T} \mid v \leq t \text{ and } t - v \leq L_p\}$, where L_p is the process-specific lifetime. The inventory becomes:

$$\boldsymbol{g}_t^{\mathrm{flex}} = \sum_{v \in \mathcal{V}_t} \boldsymbol{B}_{\delta=t-v,\,v}^{\mathrm{cap}}\, \boldsymbol{s}_v + \sum_{v \in \mathcal{V}_t^{\mathrm{op}}} \boldsymbol{B}_v^{\mathrm{op}}\, \boldsymbol{o}_{t,v} \tag{11}$$

Demand satisfaction and operational level constraints complete the formulation. The total demand $\boldsymbol{f}_t$ is met by the sum of production across all operable vintages, while each vintage's operational level is bounded by its deployed capacity:

$$\sum_{v \in \mathcal{V}_t^{\mathrm{op}}} \boldsymbol{A}_v^{\mathrm{op}}\, \boldsymbol{o}_{t,v} = \boldsymbol{f}_t \tag{12a}$$

$$\boldsymbol{o}_{t,v} \leq \boldsymbol{s}_v \quad \forall v \in \mathcal{V}_t^{\mathrm{op}} \tag{12b}$$

2.2.4 Incorporating Background Systems

The formulation developed so far is self-contained and can be used for bottom-up system modeling. However, real-world supply chains are complex, making fully bottom-up modeling impractical. In LCA and LCO practice, the system is therefore commonly divided into a foreground system and a background system. The foreground comprises the processes that are directly modeled and subject to optimization, while the background represents the broader economy and upstream supply chains that lie outside the decision maker's scope of influence. Because background systems cannot directly be influenced, their supply chains are fixed and contain no decision variables in the LCO context, and can therefor be sourced from life cycle inventory databases.

To incorporate background systems, we partition the technosphere into foreground $\boldsymbol{A}^{\mathrm{fg}}$ and background $\boldsymbol{A}^{\mathrm{bg}}$, and correspondingly the biosphere into $\boldsymbol{B}^{\mathrm{fg}}$ and $\boldsymbol{B}^{\mathrm{bg}}$. The formulation from the preceding sections applies to the foreground, with $\boldsymbol{g}_t^{\mathrm{fg,flex}}$ following directly from Eq. 11. For the background, we need to determine the inventory induced by the foreground's demand for background processes.

2.2.4.1 Background Inventory The foreground's intermediate flows to the background define the demand for background processes at time t:

$$\boldsymbol{f}_t^{\mathrm{bg}} = \sum_{v \in \mathcal{V}_t} \boldsymbol{A}^{\mathrm{cap}}_{\delta=t-v,\, v}\, \boldsymbol{s}_v + \sum_{v \in \mathcal{V}_t^{\mathrm{op}}} \boldsymbol{A}^{\mathrm{op}}_v\, \boldsymbol{o}_{t,v} \tag{13}$$

The elementary flows per unit product from a background process are captured by $\boldsymbol{\Lambda}$, the intensity matrix[34]:

$$\boldsymbol{\Lambda} = \boldsymbol{B}^{\mathrm{bg}} \left(\boldsymbol{A}^{\mathrm{bg}}\right)^{-1} \tag{14}$$

Notably, $\boldsymbol{A}^{\mathrm{bg}}$ is a square matrix (i.e., each product is produced by exactly one process in the background), thus it is invertible and contains no decision variables for the optimization.

In the simplest case, $\boldsymbol{\Lambda}$ is static and the background inventory at time t is:

$$\boldsymbol{g}_t^{\mathrm{bg}} = \boldsymbol{\Lambda}\,\boldsymbol{f}_t^{\mathrm{bg}} \tag{15}$$

2.2.4.2 Temporal Evolution through Time-Specific Background Systems A static $\boldsymbol{\Lambda}$ does not reflect that background supply chains evolve over time. To capture this, we allow demands to be fulfilled from different time-specific background systems versions $b \in \mathcal{B}$, each representing the state of the economy at a particular point in time. A mapping matrix $\boldsymbol{M}$ assigns system times t to background system version b: in the simplest case, $\boldsymbol{M}$ is an identity matrix. When background system versions are available at coarser resolution (e.g., 5-year steps) while system time t is finer resolution, $\boldsymbol{M}$ can interpolate between available versions. The background inventory from Eq. 15 then generalizes to:

$$\boldsymbol{g}_t^{\mathrm{bg}} = \left(\sum_{b\in\mathcal{B}} \boldsymbol{\Lambda}_b\,\boldsymbol{M}_{b,t}\right)\boldsymbol{f}_t^{\mathrm{bg}} \tag{16}$$

2.2.4.3 Temporal Distribution through Graph Traversal Eq. 16 assumes that all upstream background processes triggered by a foreground demand at time t also occur at t. In reality, background supply chains also encompass temporal distribution: an intermediate flow in the background may occur at a time-shifted point $t+\delta'$, where a different background system version version may apply, cascading into different elementary flow amounts upstream. To jointly capture both temporal evolution and distribution in the background, we define a temporally resolved intensity matrix $\hat{\boldsymbol{\Lambda}}_t$:

$$\boldsymbol{g}_t^{\mathrm{bg,flex}} = \hat{\boldsymbol{\Lambda}}_t\,\boldsymbol{f}_t^{\mathrm{bg}} \tag{17}$$

To construct $\hat{\boldsymbol{\Lambda}}_t$, we traverse the background system supply chains, treating them as a weighted directed graph, where time deltas δ can be defined for each edge, i.e., each intermediate or elementary flow[22,35]. For each background intermediate flow demanded at system time t, the traversal checks if a time delta δ' is defined for the specific flow, computes the absolute system time $t_n = t + \delta'$, and uses $\boldsymbol{M}$ to select the appropriate time-specific background system version to identify the next node to traverse to. When a time lag δ' is defined on a background intermediate flow, the upstream node is visited at $t_n + \delta'$, shifting which time-specific background system version applies. When no temporal distributions are defined, all upstream nodes are evaluated at the same t and the traversal reduces to Eq. 16.

2.2.4.4 Combined Inventory and Impact With both foreground and background inventories determined, the environmental impact at time t is:

$$h_t^{\mathrm{c}} = \boldsymbol{Q}_t^{\mathrm{c}} \left(\boldsymbol{g}_t^{\mathrm{fg,flex}} + \boldsymbol{g}_t^{\mathrm{bg,flex}} \right) \tag{18}$$

2.2.5 Complete Optimization Problem Formulation

Combining all elements, the complete time-explicit LCO problem is:

$$\min_{\boldsymbol{s}_v,\, \boldsymbol{o}_{t,v}} \quad \sum_{t \in \mathcal{T}} \boldsymbol{Q}_t^{\mathrm{c}} \left(\boldsymbol{g}_t^{\mathrm{fg,flex}} + \boldsymbol{g}_t^{\mathrm{bg,flex}} \right) \tag{19a}$$

$$\text{s.t.} \quad \boldsymbol{o}_{t,v} \leq \boldsymbol{s}_v \quad \forall t \in \mathcal{T}, v \in \mathcal{V}_t^{\mathrm{op}}, \tag{19b}$$

$$\sum_{v \in \mathcal{V}_t^{\mathrm{op}}} \boldsymbol{A}_v^{\mathrm{op}}\, \boldsymbol{o}_{t,v} = \boldsymbol{f}_t \quad \forall t \in \mathcal{T}, \tag{19c}$$

$$\boldsymbol{s}_v \geq \boldsymbol{0} \quad \forall v \in \mathcal{T}, \quad \boldsymbol{o}_{t,v} \geq \boldsymbol{0} \quad \forall t \in \mathcal{T}, v \in \mathcal{V}_t^{\mathrm{op}}. \tag{19d}$$

2.3 Operationalization

We now describe how to operationalize the proposed mathematical framework for time-explicit LCO, detailing the steps required to implement the framework in practice (see Fig. 1). First, we explain how foreground systems are modeled, including the temporal information, the differentiation of installation- and operation-dependent flows, and vintage-specific evolution (Section 2.3.1). Next, we detail how time-specific values are inserted into time-explicit matrices (Section 2.3.2). Finally, we outline how the final optimization problem is composed (Section 2.3.3).

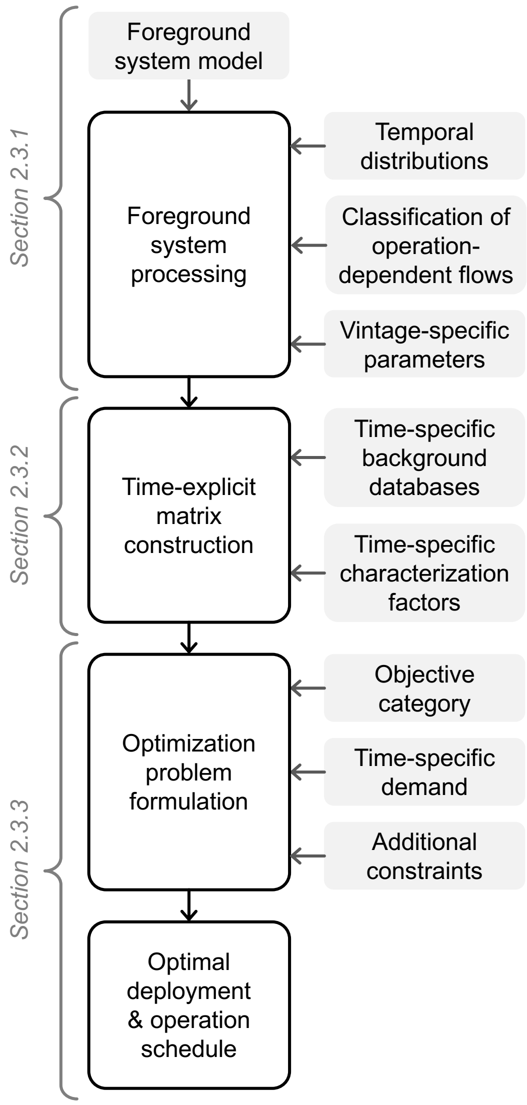

Figure 1: Time-explicit LCO workflow.

2.3.1 Preparing the Foreground System

The first step of a time-explicit LCO is to prepare the foreground system including the set of possible processes to install and operate. As in conventional LCA or LCO, this begins with modeling the product system by defining products, processes, and their intermediate and elementary flows. Building on this product system model, the preparation then involves three additional tasks. First, we embed temporal information in the product system model, reflecting the temporal distributions of intermediate and elementary flows. To achieve this, process-relative temporal distributions (rTDs) are used, following the approach introduced by Beloin-Saint-Pierre et al.[20] and implemented by Cardellini et al.[22]. These rTDs define what share of an intermediate or elementary flow occurs at what time delta, with respect to the consuming or emitting process. The underlying temporal resolution of rTDs is flexible, and can range from hourly to yearly values. Second, we mark operation-dependent flows so they can be scaled separately from capacity installation. Third, to reflect the temporal evolution of foreground processes through vintage-dependent parameters (cf. Eq. 10), technology evolution can be specified as a mapping from absolute system times t to time-specific scaling factors ϕ for each intermediate and elementary flow.

2.3.2 Constructing Time-explicit Matrices

The temporalized foreground system from the previous step is then combined with two additional inputs, time-specific background databases and time-specific characterization factors, to construct the full set of time-explicit matrices (Fig. 1).

For the foreground, the rTDs, operation-dependent flow classifications, and vintage-specific scaling factors are translated into the time-explicit technosphere and biosphere matrices. The rTDs determine the distribution of each flow across process time steps δ. The operation-dependent flow classification splits these into capacity matrices ($\boldsymbol{A}_{\delta,v}^{\mathrm{cap}}$, $\boldsymbol{B}_{\delta,v}^{\mathrm{cap}}$) and operation matrices ($\boldsymbol{A}_{v}^{\mathrm{op}}$, $\boldsymbol{B}_{v}^{\mathrm{op}}$). The vintage-specific scaling factors are then applied to the corresponding coefficients.

For the background, time-specific databases representing the state of background production systems at specific absolute points in time are used to construct the intensity matrices $\boldsymbol{\Lambda}_b$ (Eq. 14). Users can create such databases based on their own assumptions or external scenarios, e.g., using tools like `premise`[25]. The temporal resolution of the background databases is not required to match the temporal resolution of the rTDs, as the mapping matrix $\boldsymbol{M}$ bridges the two resolutions.

Finally, time-specific characterization factors populate the characterization matrices

$\boldsymbol{Q}_t$. The framework is agnostic to the source of these factors and applicable across impact categories where timing matters, including climate change, water use[36], toxicity[37], or noise[38]. For climate change, for example, dynamic LCIA methods can provide dynamic metrics such as Radiative Forcing (RF), Absolute Global Warming Potential (AGWP, i.e., the cumulative RF over time), or Absolute Global Temperature Change Potential (AGTP), or prospective-dynamic metrics such as prospective AGWP and AGTP as recently proposed by Watanabe and Cherubini[39]. Alternatively, static characterization factors can be used when temporal differentiation is not required for a given impact category.

2.3.3 Defining Objectives and Constraints

To set up the optimization problem, we choose an objective, which can be any environmental impact category and metric. Next, the user defines a time-specific demand, specifying product amounts and the points in time at which they are required. This demand can be expressed as an rTD with respect to a user-defined (absolute) reference time. Together with the time-explicit LCA matrices introduced above, these inputs parameterize the optimization model in Eq. 19. Optionally, further constraints can be added, such as existing (brownfield) process capacities and stock- or flow-related limits on process installations, environmental impact categories, or individual intermediate or elementary flows.

2.4 Implementation

The proposed time-explicit LCO framework is implemented in the open-source Python package `optimex`[40]. For LCA-related capabilities, `optimex` builds on the open-source LCA framework `Brightway`[32] and shares a common temporal modeling approach with the time-explicit LCA package `bw_timex`[41]. For dynamic LCIA, `optimex` directly sources methods from the `Brightway` library `dynamic_characterization`[42]. For optimization, `optimex` uses the open-source optimization framework `pyomo`[33]. Additional information and instructions are available in the comprehensive online documentation of `optimex`[43]. Together, these components allow practitioners to set up time-explicit LCO problems using familiar LCA and optimization workflows.

3 Application

To demonstrate the capabilities of time-explicit LCO, we apply the proposed framework to an integrated industrial system co-producing methanol and pig iron through a combination of conventional and novel technologies. This case study illustrates methodological capabilities rather than comprehensively assessing methanol and pig iron production systems. Section 3.1 describes the production system and optimization setup following the previously described workflow (see Fig 1). Section 3.2 presents the case study results. The full case study code is available as an annotated Jupyter Notebook in the `optimex` GitHub repository[40].

3.1 Case Study Setup

As the foreground system that is subject to optimization, we consider a production system for methanol and pig iron (Fig. 2).

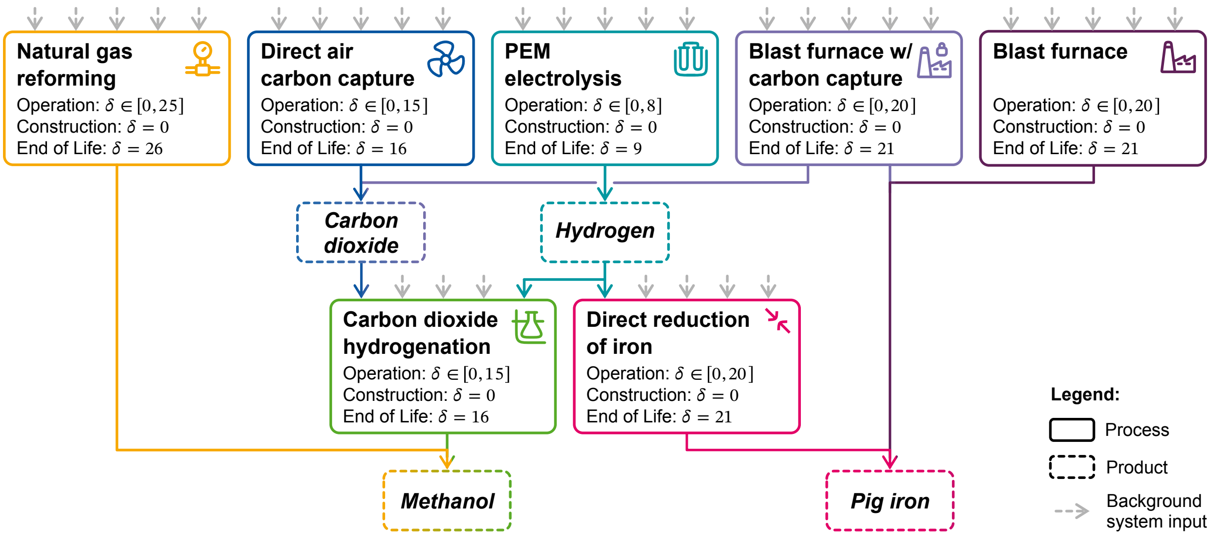

Figure 2: Production system for methanol and pig iron.

The production system must meet a constant annual demand of 1 Mt methanol and 1 Mt pig iron from 2025 to 2050. We model this as a brownfield optimization problem, accounting for existing fossil-based production infrastructure. We assume that 0.5 Mt of yearly capacity was installed in both 2005 and 2015 for both methanol (via natural gas reforming) and pig iron (via standard blast furnace), totaling 1 Mt of legacy capacity at the start of the transition period.

From the beginning of the transition period in 2025, the system can draw on additional process and supply chain choices to satisfy the demands. For methanol synthesis, the model can choose between conventional natural gas (NG) reforming (lifetime $L = 25$ years) and CO_2 hydrogenation ($L = 15$ years). The latter offers flexible CO_2 sourcing, either from point-source capture via a blast furnace with carbon capture (BF-CC) or from atmospheric removal via direct air carbon capture (DAC). Similarly, pig iron production is diversified through standard blast furnaces, BF-CC, and hydrogen-based direct reduction of iron (H_2-DRI). These production routes are highly intertwined: the BF-CC process co-produces pig iron and the CO_2 feedstock for methanol synthesis, while Proton Exchange Membrane (PEM) electrolysis ($L = 8$ years) provides the hydrogen required for both CO_2 hydrogenation and the H_2-DRI route. Each process is associated with specific installation- and operation-dependent intermediate and elementary flows, distributed across distinct time-relative phases: construction ($\delta \leq 0$), operation ($\delta \in [0, L]$), and end-of-life treatment ($\delta > L$). We derive process-specific inventories from the ecoinvent 3.12 database[44].

With the foreground system defined, we specify the optimization objective and LCIA methods. We minimize climate impacts, assessed through the dynamic AGWP with a fixed end year of 2125 for all emissions. The dynamic AGWP corresponds to the cumulative RF over time, i.e., the total energy commitment to the atmosphere caused by the inventory. For further analysis of climate impacts, we additionally assess the underlying instantaneous RF. This instantaneous RF represents the actual warming rate at a specific point in time, including the effect of previous emissions that have partially decayed until then. As an additional impact category, we consider the water use impact, which we assess through static characterization factors from Environmental Footprint 3.1[45]

To demonstrate the framework's versatility, we define three modeling scenarios. The "Baseline" scenario has no temporal evolution, i.e., foreground parameters and background supply chains are fixed at 2025 states. The "Evolution" scenario assumes continuous improvement in both the foreground and the background system. In the foreground, efficiency gains are modeled through vintage-dependent scaling factors, including decreasing electricity consumption for PEM electrolysis, decreasing electricity and heat consumption for DAC, and decreasing electricity consumption and reduced direct fugitive CO_2 emissions for the CO_2 hydrogenation process. For the background sytem, we assume extensive decarbonization. We utilize a set of prospective ecoinvent 3.12 databases[44] modified according to the REMIND-EU IAM[46] in the SSP2-NDC scenario. This scenario reflects "middle of the road" socioeconomic developments with climate targets following Nationally Determined Contributions (NDCs), leading to below 2.5°C warming by 2100. The prospective databases cover the period from 2020 to 2100 and are created via `premise` (version 2.3.4)[25]. Finally, the "Constrained Evolution" scenario introduces resource bottlenecks on top of the Evolution scenario, including a flow-related annual limit on water use impact ($3 \cdot 10^5$ m^3-eq) and a stock-related cumulative limit on Iridium extraction (0.125 kg) as a proxy for critical mineral scarcity.

All further modeling details and assumptions are available in an annotated Jupyter Notebook in the `optimex` GitHub repository[40].

3.2 Results

The time-explicit LCO results for the integrated methanol and pig iron production system across scenarios are summarized in Fig. 3.

In the Baseline scenario (Fig. 3 a-1 to g-1), the model identifies no incentive for technological change, maintaining fossil-based natural gas reforming and blast furnaces through 2050. The installed capacity (dashed lines) exactly matches the demand, representing

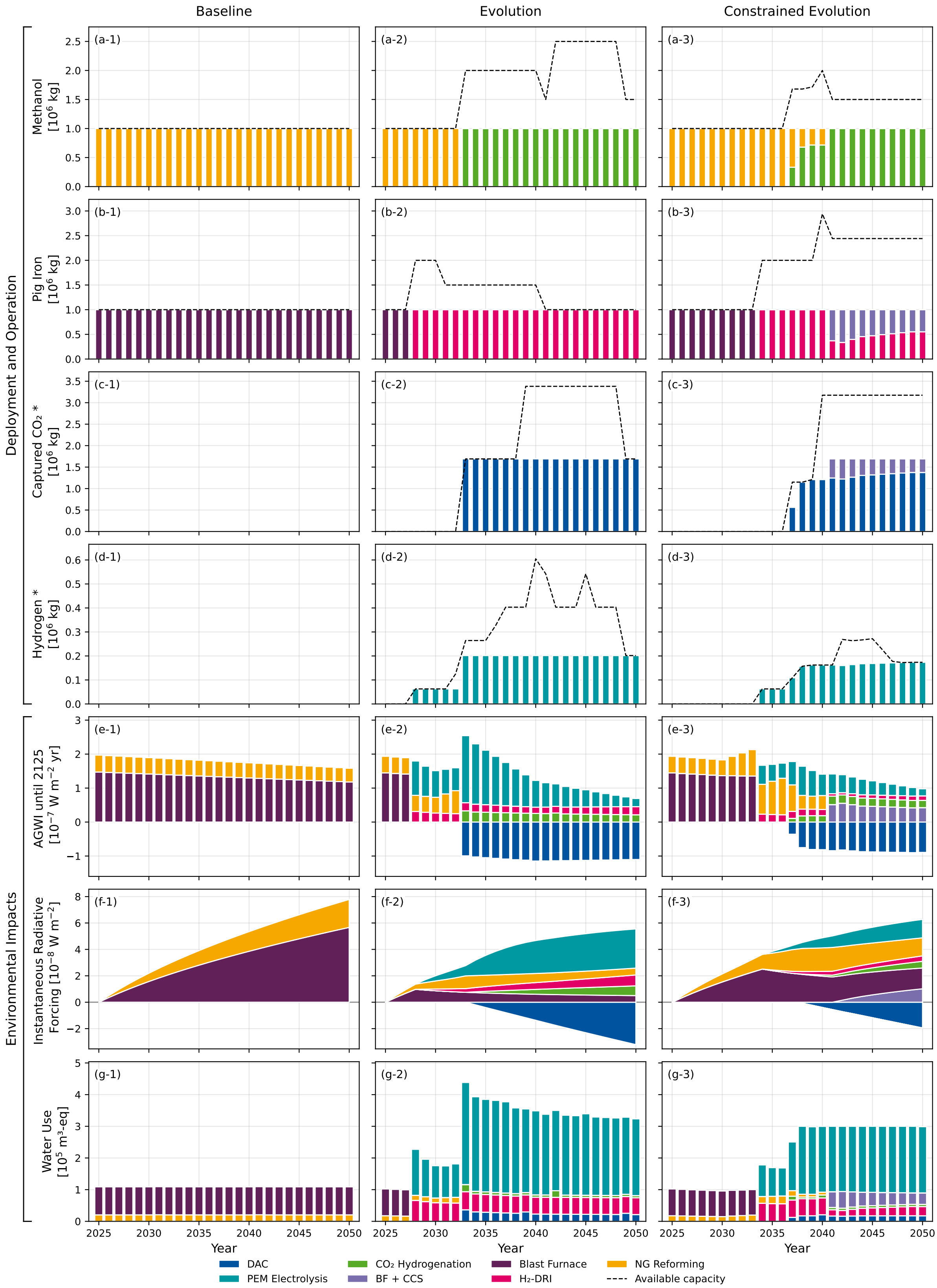

Figure 3: Installation, operation and environmental impacts of the optimized methanol and pig iron production system over the transition pathway. Asterisks indicate intermediate products.

100% utilization of installed capacity. Once installed capacities reach the end of their lifetime, new capacities are immediately installed to replace them. Fig. 3 e-1 shows the resulting climate impact through the annual Absolute Global Warming Impact (AGWI). The AGWI bars represent the warming impact of the emissions occuring in each year, integrated over the remaining time until 2125. For the Baseline scenario, the annual AGWI declines over time. This decline is a consequence of the fixed 2125-time horizon: later emissions contribute to warming over a shorter remaining duration, so their impact is effectively reduced. In contrast, the instantaneous RF curves (f-1) depict the actual warming rate caused by the inventory. While these curves rise, their slope flattens over time. This flattening is driven by the atmospheric decay of greenhouse gases: as the inventory accumulates, the radiative forcing lost to the decay of past emissions increasingly counteracts the forcing added by new emissions, causing the net growth rate to slow. For water use, the impact remains constant throughout the period (g-1) because we use static characterization factors.

In the Evolution scenario (Fig. 3 a-2 to g-2), the model identifies a phased transition toward electrification starting in 2033. As background electricity impacts decrease, the system switches to CO_2 hydrogenation for methanol and H_2-DRI for pig iron. Overcapacities emerge (dashed lines exceeding solid bars): the model finds that switching earlier to electrification routes, and the resulting savings in operational emissions, outweighs the impacts of idled fossil-based brownfield capacities. Beyond these capacity decisions, the scenario reveals how technology improvement shapes climate trajectories (Fig. 3 e-2, f-2). For instance, for electrolysis, even when production levels remain constant after 2033 (d-2), the yearly AGWI bars decline due to the decarbonization of background inputs and efficiency improvements. Compared to the Baseline scenario (e-1), where the decline stems solely from the decreasing integration horizon, the Evolution scenario shows a more pronounced decrease. Accordingly, the slope of the corresponding instantaneous RF curves (f-2) also decreases as cleaner production vintages are preferentially operated later, idling previously built and still operable installations.

Finally, the Constrained Evolution scenario (Fig. 3 a-3 to g-3) demonstrates the framework's ability to navigate resource bottlenecks. The previous evolution scenario revealed that hydrogen-based routes carry substantial water impacts (g-2). By imposing annual water availability caps and a cumulative limit on Iridium for which mostly affect the PEM, the model is forced to diversify its technological portfolio. The system shifts back toward a mix of technologies in later years, utilizing BF-CC for iron production to stay within resource limits, but slightly raising climate impacts.

Overall, these results illustrate that time-explicit LCO identifies transition pathways that navigate complex temporal interdependencies hidden in static assessments. By resolving these interdependencies, the framework reveals trade-offs such as strategic overcapacities with preferential operation of cleaner vintages, and navigates transient resource bottlenecks through technology diversification. These capabilities remain inaccessible to models that collapse all flows to a single point in time.

4 Discussion

Designing sustainable transition pathways that respect environmental constraints requires optimization models capable of capturing when exchanges with the environment occur, not just their aggregated magnitudes. The time-explicit LCO framework presented in this work addresses this requirement by integrating the temporal distribution of life cycle stages and evolution of production systems into optimization models. Whereas existing LCO approaches either neglect time entirely or only account for prospective changes in background systems, our framework tracks the full temporal profile of both intermediate and elementary flows across life cycles and supply chains, while simultaneously reflecting technological progress and economy-wide decarbonization.

4.1 Relevance of Time-Explicit Life Cycle Optimization

The case study (Section 3.2) demonstrates how the interplay between installation timing, operational emissions, and technological evolution leads to transition pathways that differ substantially from static approaches. Capabilities inaccessible to static approaches emerge: the framework identifies hidden trade-offs, such as strategic overcapacities where early investment in cleaner technologies outweighs embodied infrastructure impacts and newer vintages are preferentially operated, and navigates transient resource bottlenecks by diversifying technology portfolios.

These capabilities depend not only on temporal resolution in the inventory but also on the choice of impact assessment method. The framework supports both static and dynamic LCIA, with the latter necessary for capturing time-sensitive impacts. For climate change, dynamic metrics such as RF are essential when considering the different atmospheric lifetimes of greenhouse gases and their time-dependent energy absorptions. Beyond climate change, the framework extends to other impact categories where timing matters, such as water use[36], toxicity[37], or noise[38].

Time-explicit LCO is broadly relevant across sectors where temporal dynamics are decisive, for example: (1) systems depending on evolving upstream processes, where inputs such as electricity, steel, or hydrogen undergo rapid decarbonization; (2) early-stage technologies with steep learning curves, where vintage-dependent performance gains are significant; (3) circular economy planning with long material residence times, where decades-long lags between installation and end-of-life create temporal mismatches between primary demand and secondary supply; (4) time-resolved carbon accounting, such as biogenic feedstocks with varying rotation periods, temporary carbon storage in CO_2-based products, or carbon dioxide removal technologies with varying temporal profiles for CO_2 removals; (5) the built environment, where long service lives create substantial temporal mismatches between construction, operation, and end-of-life impacts; and (6) multi-regional supply chains with divergent evolution, where sourcing decisions must account for heterogeneous decarbonization trajectories across production regions alongside region-specific total availabilities. Across these applications, the framework's temporal resolution is fully flexible: while the case study demonstrates yearly resolution, seasonal resolution can capture water availability constraints, and hourly resolution can reflect the diurnal availability of renewable electricity.

To facilitate the application of time-explicit LCO, we provide an open-source implementation in the Python package `optimex`[40], building on the `Brightway` LCA framework[32] and the `pyomo` optimization framework[33]. Users can leverage familiar LCA modeling approaches to define production systems, and then extend them with rTDs, vintage-dependent evolution factors, and the classification of installation and operation-dependent flows, enabling independent scaling of infrastructure required for vintage-specific process operation. By natively integrating time-specific databases from `premise`[25] and dynamic characterization functions from `dynamic_characterization`[42], `optimex` automatically constructs the optimization model from these inputs, allowing practitioners to focus on process and system modeling.

4.2 Extensions and Future Directions

The framework's mathematical structure lends itself to several extensions, spanning economic objectives, circular economy modeling, and advanced optimization techniques.

In practice, most real-world transition pathway optimization is driven by economics rather than environmental objectives alone. Adapting the proposed framework to cost minimization is straightforward: the environmental objective in Eq. 19 can be replaced by a cost objective (cf. Kätelhön et al.[16]), while time-explicit environmental targets are enforced as constraints. Technology-specific cost parameters, including capital expenditures, operational costs, and feedstock prices, can be incorporated as time-dependent coefficients, analogous to the vintage-dependent scaling factors (Eq. 10). The model can then reflect projected cost reductions from learning curves, evolving energy prices, or shifting raw material costs.

Beyond general cost parameters, the ability to resolve exact emission timing has specific implications for carbon markets, where emissions are typically priced using static metrics like GWP100, irrespective of when they occur. Yet, as carbon prices are projected to rise, emission costs become time-dependent. Time-explicit LCO could integrate such price trajectories directly, enabling optimization that minimizes financial risk alongside environmental impact. This integration is particularly relevant for sectors with long-lived infrastructure, where decisions to delay construction or prioritize early operational savings yield vastly different economic outcomes.

Alongside economic extensions, the framework provides a foundation for modeling circular economy dynamics. Internal material circularity in the foreground system can already be represented: secondary materials from end-of-life activities of earlier vintages enter product balances at specific system times, becoming available for subsequent installation phases. This representation, for example, enables pathways that optimize recycling loops within primary resource extraction limits. Such internal modeling could be complemented by interfacing with dynamic material flow analysis[47], allowing stocks and flows external to the system boundary to be accounted for and providing more comprehensive constraints on resource availability[29,48].

Finally, by formulating time-explicit LCO as a mathematical optimization problem, the framework opens access to a broad range of established optimization methods. Future work can leverage multi-objective optimization to reveal trade-offs, or near-optimal methods to identify diverse pathways that align with political feasibility. Additionally, stochastic programming can ensure robustness against uncertainty, while mixed-integer and non-linear formulations capture discrete investments and economies of scale, collectively refining time-explicit LCO as a tool for strategic planning of sustainable transitions.

References

[1] Johan Rockström, Will Steffen, Kevin Noone, Åsa Persson, F. Stuart Chapin, Eric F. Lambin, Timothy M. Lenton, Marten Scheffer, Carl Folke, Hans Joachim Schellnhuber, Björn Nykvist, Cynthia A. de Wit, Terry Hughes, Sander van der Leeuw, Henning Rodhe, Sverker Sörlin, Peter K. Snyder, Robert Costanza, Uno Svedin, Malin Falkenmark, Louise Karlberg, Robert W. Corell, Victoria J. Fabry, James Hansen, Brian Walker, Diana Liverman, Katherine Richardson, Paul Crutzen, and Jonathan A. Foley. A safe operating space for humanity. *Nature*, 461(7263):472–475, September 2009. ISSN 1476-4687. doi: 10.1038/461472a.

[2] Will Steffen, Katherine Richardson, Johan Rockström, Sarah E. Cornell, Ingo Fetzer, Elena M. Bennett, Reinette Biggs, Stephen R. Carpenter, Wim de Vries, Cynthia A. de Wit, Carl Folke, Dieter Gerten, Jens Heinke, Georgina M. Mace, Linn M. Persson, Veerabhadran Ramanathan, Belinda Reyers, and Sverker Sörlin. Planetary boundaries: Guiding human development on a changing planet. *Science*, 347(6223): 1259855, February 2015. doi: 10.1126/science.1259855.

[3] International Energy Agency. Global Critical Minerals Outlook 2025 – Analysis. https://www.iea.org/reports/global-critical-minerals-outlook-2025, May 2025.

[4] Intergovernmental Panel On Climate Change (Ipcc). *Climate Change 2021 – The Physical Science Basis: Working Group I Contribution to the Sixth Assessment Report of the Intergovernmental Panel on Climate Change*. Cambridge University Press, 1 edition, July 2023. ISBN 978-1-009-15789-6. doi: 10.1017/9781009157896.

[5] Joeri Rogelj, Piers M. Forster, Elmar Kriegler, Christopher J. Smith, and Roland Séférian. Estimating and tracking the remaining carbon budget for stringent climate targets. *Nature*, 571(7765):335–342, July 2019. ISSN 1476-4687. doi: 10.1038/s41586-019-1368-z.

[6] Gwenny Thomassen, Adithya Eswaran, Steven Van Passel, and Jo Dewulf. A Plan-

etary Boundary for Mineral, Metal, and Fossil Resource Extraction Rates: How Much Primary Materials Can a Circular Economy Extract? *Environmental Science & Technology*, 58(46):20345–20351, November 2024. ISSN 0013-936X. doi: 10.1021/acs.est.4c08688.

[7] John Weyant. Some Contributions of Integrated Assessment Models of Global Climate Change. *Review of Environmental Economics and Policy*, 11(1):115–137, January 2017. ISSN 1750-6816. doi: 10.1093/reep/rew018.

[8] Stefan Pauliuk, Anders Arvesen, Konstantin Stadler, and Edgar G. Hertwich. Industrial ecology in integrated assessment models. *Nature Climate Change*, 7(1):13–20, January 2017. ISSN 1758-678X, 1758-6798. doi: 10.1038/nclimate3148.

[9] Pénélope Bieuville, Guillaume Majeau-Bettez, and Anne De Bortoli. Technology flexibility and sobriety to address shortage of energy-transition metals. *Nature Sustainability*, January 2026. ISSN 2398-9629. doi: 10.1038/s41893-025-01762-y.

[10] Marte Fodstad, Pedro Crespo del Granado, Lars Hellemo, Brage Rugstad Knudsen, Paolo Pisciella, Antti Silvast, Chiara Bordin, Sarah Schmidt, and Julian Straus. Next frontiers in energy system modelling: A review on challenges and the state of the art. *Renewable and Sustainable Energy Reviews*, 160:112246, May 2022. ISSN 1364-0321. doi: 10.1016/j.rser.2022.112246.

[11] Christiane Reinert, Lars Schellhas, Jacob Mannhardt, David Yang Shu, Andreas Kämper, Nils Baumgärtner, Sarah Deutz, and André Bardow. SecMOD: An Open-Source Modular Framework Combining Multi-Sector System Optimization and Life-Cycle Assessment. *Frontiers in Energy Research*, 10, June 2022. ISSN 2296-598X. doi: 10.3389/fenrg.2022.884525.

[12] Carla Pieragostini, Miguel C. Mussati, and Pío Aguirre. On process optimization considering LCA methodology. *Journal of Environmental Management*, 96(1):43–54, April 2012. ISSN 0301-4797. doi: 10.1016/j.jenvman.2011.10.014.

[13] Herib Blanco, Victor Codina, Alexis Laurent, Wouter Nijs, François Maréchal, and André Faaij. Life cycle assessment integration into energy system models: An application for Power-to-Methane in the EU. *Applied Energy*, 259:114160, February 2020. ISSN 0306-2619. doi: 10.1016/j.apenergy.2019.114160.

[14] Jannatul Ferdous, Farid Bensebaa, and Nathan Pelletier. Integration of LCA, TEA, Process Simulation and Optimization: A systematic review of current practices and scope to propose a framework for pulse processing pathways. *Journal of Cleaner Production*, 402:136804, May 2023. ISSN 0959-6526. doi: 10.1016/j.jclepro.2023.136804.

[15] Adisa Azapagic and Roland Clift. Linear programming as a tool in life cycle assessment. *The International Journal of Life Cycle Assessment*, 3(6):305–316, November 1998. ISSN 1614-7502. doi: 10.1007/BF02979340.

[16] Arne Kätelhön, André Bardow, and Sangwon Suh. Stochastic Technology Choice Model for Consequential Life Cycle Assessment. *Environmental Science & Technology*, 50(23):12575–12583, December 2016. ISSN 0013-936X. doi: 10.1021/acs.est.6b04270.

[17] Fabian Lechtenberg, Robert Istrate, Victor Tulus, Antonio Espuña, Moisès Graells, and Gonzalo Guillén-Gosálbez. PULPO: A framework for efficient integration of life cycle inventory models into life cycle product optimization. *Journal of Industrial Ecology*, n/a(n/a), 2024. ISSN 1530-9290. doi: 10.1111/jiec.13561.

[18] Amelie Müller, Timo Diepers, Arthur Jakobs, Giuseppe Cardellini, Niklas von der Assen, Jeroen Guinée, and Bernhard Steubing. Time-explicit life cycle assessment: A flexible framework for coherent consideration of temporal dynamics. *The International Journal of Life Cycle Assessment*, October 2025. ISSN 1614-7502. doi: 10.1007/s11367-025-02539-3.

[19] William O. Collinge, Amy E. Landis, Alex K. Jones, Laura A. Schaefer, and

Melissa M. Bilec. Dynamic life cycle assessment: Framework and application to an institutional building. *The International Journal of Life Cycle Assessment*, 18 (3):538–552, March 2013. ISSN 1614-7502. doi: 10.1007/s11367-012-0528-2.

[20] Didier Beloin-Saint-Pierre, Reinout Heijungs, and Isabelle Blanc. The ESPA (Enhanced Structural Path Analysis) method: A solution to an implementation challenge for dynamic life cycle assessment studies. *The International Journal of Life Cycle Assessment*, 19(4):861–871, April 2014. ISSN 1614-7502. doi: 10.1007/s11367-014-0710-9.

[21] Ligia Tiruta-Barna, Yoann Pigné, Tomás Navarrete Gutiérrez, and Enrico Benetto. Framework and computational tool for the consideration of time dependency in Life Cycle Inventory: Proof of concept. *Journal of Cleaner Production*, 116:198–206, March 2016. ISSN 0959-6526. doi: 10.1016/j.jclepro.2015.12.049.

[22] Giuseppe Cardellini, Christopher L. Mutel, Estelle Vial, and Bart Muys. Temporalis, a generic method and tool for dynamic Life Cycle Assessment. *Science of The Total Environment*, 645:585–595, December 2018. ISSN 00489697. doi: 10.1016/j.scitotenv.2018.07.044.

[23] Benedikt M Zimmermann, Hanna Dura, Manuel J Baumann, and Marcel R Weil. Prospective time-resolved LCA of fully electric supercap vehicles in Germany. *Integrated Environmental Assessment and Management*, 11(3):425–434, July 2015. ISSN 1551-3777. doi: 10.1002/ieam.1646.

[24] Angelica Mendoza Beltran, Brian Cox, Chris Mutel, Detlef P. van Vuuren, David Font Vivanco, Sebastiaan Deetman, Oreane Y. Edelenbosch, Jeroen Guinée, and Arnold Tukker. When the Background Matters: Using Scenarios from Integrated Assessment Models in Prospective Life Cycle Assessment. *Journal of Industrial Ecology*, 24(1):64–79, 2020. ISSN 1530-9290. doi: 10.1111/jiec.12825.

[25] R. Sacchi, T. Terlouw, K. Siala, A. Dirnaichner, C. Bauer, B. Cox, C. Mutel, V. Daioglou, and G. Luderer. PRospective EnvironMental Impact asSEment (*premise*): A streamlined approach to producing databases for prospective life cycle assessment using integrated assessment models. *Renewable and Sustainable Energy Reviews*, 160:112311, May 2022. ISSN 1364-0321. doi: 10.1016/j.rser.2022.112311.

[26] Christiane Reinert, Sarah Deutz, Hannah Minten, Lukas Dörpinghaus, Sarah Von Pfingsten, Nils Baumgärtner, and André Bardow. Environmental impacts of the future German energy system from integrated energy systems optimization and dynamic life cycle assessment. *Computers & Chemical Engineering*, 153:107406, October 2021. ISSN 00981354. doi: 10.1016/j.compchemeng.2021.107406.

[27] Margarita A. Charalambous, Daniel Vázquez, Ana I. Torres, and Gonzalo Guillén-Gosálbez. The underrepresented role of prospective global supply chains in the life cycle optimization of energy systems. *Renewable and Sustainable Energy Reviews*, 233:116829, June 2026. ISSN 13640321. doi: 10.1016/j.rser.2026.116829.

[28] Vyom Thakker and Bhavik R. Bakshi. Mapping the path to a net-zero chemicals industry by long-term planning with changes in technologies and climate. *AIChE Journal*, 70(5):e18381, May 2024. ISSN 0001-1541, 1547-5905. doi: 10.1002/aic.18381.

[29] Christine Roxanne Hung, Paul Kishimoto, Volker Krey, Anders Hammer Strømman, and Guillaume Majeau-Bettez. ECOPT2: An adaptable life cycle assessment model for the environmentally constrained optimization of prospective technology transitions. *Journal of Industrial Ecology*, 26(5):1616–1630, 2022. ISSN 1530-9290. doi: 10.1111/jiec.13331.

[30] Ladislaus Lang-Quantzendorff and Martin Beermann. Time-differentiating methods for life cycle assessment of the industry transition toward climate neutrality: A

review. *Journal of Industrial Ecology*, 29(5):1523–1550, October 2025. ISSN 1088-1980, 1530-9290. doi: 10.1111/jiec.70068.

[31] I. Turner, N. Bamber, J. Andrews, and N. Pelletier. Systematic review of the life cycle optimization literature, and recommendations for performance of life cycle optimization studies. *Renewable and Sustainable Energy Reviews*, 208:115058, February 2025. ISSN 1364-0321. doi: 10.1016/j.rser.2024.115058.

[32] Chris Mutel. Brightway: An open source framework for Life Cycle Assessment. *Journal of Open Source Software*, 2(12):236, April 2017. ISSN 2475-9066. doi: 10.21105/joss.00236.

[33] Michael L. Bynum, Gabriel A. Hackebeil, William E. Hart, Carl D. Laird, Bethany L. Nicholson, John D. Siirola, Jean-Paul Watson, and David L. Woodruff. *Pyomo — Optimization Modeling in Python*, volume 67 of *Springer Optimization and Its Applications*. Springer International Publishing, Cham, 2021. ISBN 978-3-030-68927-8 978-3-030-68928-5. doi: 10.1007/978-3-030-68928-5.

[34] Reinout Heijungs and Sangwon Suh. *The Computational Structure of Life Cycle Assessment*. Number volume 11 in Eco-Efficiency in Industry and Science. Springer-Science+Business Media B.V, Dordrecht, 2002. ISBN 978-94-015-9900-9. doi: 10.1007/978-94-015-9900-9.

[35] Brandon Kuczenski. Partial ordering of life cycle inventory databases. *The International Journal of Life Cycle Assessment*, 20(12):1673–1683, December 2015. ISSN 1614-7502. doi: 10.1007/s11367-015-0972-x.

[36] Montserrat Núñez, Stephan Pfister, Mar Vargas, and Assumpció Antón. Spatial and temporal specific characterisation factors for water use impact assessment in Spain. *The International Journal of Life Cycle Assessment*, 20(1):128–138, January 2015. ISSN 1614-7502. doi: 10.1007/s11367-014-0803-5.

[37] Allan Hayato Shimako, Ligia Tiruta-Barna, and Aras Ahmadi. Operational integration of time dependent toxicity impact category in dynamic LCA. *Science of The Total Environment*, 599–600:806–819, December 2017. ISSN 0048-9697. doi: 10.1016/j.scitotenv.2017.04.211.

[38] S. Cucurachi and R. Heijungs. Characterisation factors for life cycle impact assessment of sound emissions. *Science of The Total Environment*, 468–469:280–291, January 2014. ISSN 0048-9697. doi: 10.1016/j.scitotenv.2013.07.080.

[39] Marcos D. B. Watanabe and Francesco Cherubini. Prospective Characterization Factors for Assessing Climate Change Impacts in Life Cycle Assessments. *Environmental Science & Technology*, page acs.est.5c12391, January 2026. ISSN 0013-936X, 1520-5851. doi: 10.1021/acs.est.5c12391.

[40] Timo Diepers and Jan Tautorus. Optimex. https://github.com/RWTH-LTT/optimex, 2026.

[41] Timo Diepers, Amelie Müller, and Arthur Jakobs. Bw_timex: A Python Package for Time-Explicit Life Cycle Assessment. *Journal of Open Source Software*, 11(120): 9621, April 2026. ISSN 2475-9066. doi: 10.21105/joss.09621.

[42] Brightway. Dynamic_characterization. https://github.com/brightway-lca/dynamic_characterization, October 2025.

[43] Timo Diepers and Jan Tautorus. Optimex documentation: Time-explicit Life Cycle Optimization for Transition Pathways. https://optimex.readthedocs.io, December 2025.

[44] Gregor Wernet, Christian Bauer, Bernhard Steubing, Jürgen Reinhard, Emilia Moreno-Ruiz, and Bo Weidema. The ecoinvent database version 3 (part I): Overview and methodology. *The International Journal of Life Cycle Assessment*, 21(9):1218–1230, September 2016. ISSN 1614-7502. doi: 10.1007/s11367-016-1087-8.

[45] Joint Research Centre (European Commission). *Updated Characterisation and Normalisation Factors for the Environmental Footprint 3.1 Method*. Publications Office of the European Union, 2023. ISBN 978-92-76-99069-7.

[46] Gunnar Luderer, Nico Bauer, Lavinia Baumstark, Christoph Bertram, Marian Leimbach, Robert Pietzcker, Jessica Strefler, Tino Aboumahboub, Gabriel Abrahão, Cornelia Auer, David Bantje, Felicitas Beier, Falk Benke, Stephen Bi, Jan Philipp Dietrich, Alois Dirnaichner, Tabea Dorndorf, Jakob Duerrwaechter, Sophie Fuchs, Pascal Führlich, Anastasis Giannousakis, Chen Chris Gong, Alex Hagen, Markus Haller, Robin Hasse, Léa Hayez, Jerome Hilaire, Verena Hofbauer, Johanna Hoppe, David Klein, Johannes Koch, Laurin Köhler-Schindler, Alexander Körner, Katarzyna Kowalczyk, Elmar Kriegler, Fabrice Lécuyer, Antoine Levesque, Alexander Lorenz, Sylvie Ludig, Michael Lüken, Aman Malik, Rahel Mandaroux, Susanne Manger, Anne Merfort, Leon Merfort, Simón Moreno-Leiva, Ioanna Mouratiadou, Jarusch Müßel, Adrian Odenweller, Michaja Pehl, Mika Pflüger, Franziska Piontek, Laura Popin, Sebastian Rauner, Oliver Richters, Renato Rodrigues, Niklas Roming, Ricarda Rosemann, Marianna Rottoli, Tonn Rüter, Robert Salzwedel, Pascal Sauer, Eva Schmidt, Christof Schötz, Felix Schreyer, Anselm Schultes, Joanna Sitarz, Björn Sörgel, Falko Ueckerdt, Philipp Verpoort, Pascal Weigmann, and Bennet Weiss. REMIND - REgional Model of INvestments and Development, April 2025.

[47] Felix Kullmann, Peter Markewitz, Detlef Stolten, and Martin Robinius. Combining the worlds of energy systems and material flow analysis: A review. *Energy, Sustainability and Society*, 11(1):13, April 2021. ISSN 2192-0567. doi: 10.1186/s13705-021-00289-2.

[48] Jiyao Gao and Fengqi You. Dynamic Material Flow Analysis-Based Life Cycle Optimization Framework and Application to Sustainable Design of Shale Gas Energy Systems. *ACS Sustainable Chemistry & Engineering*, 6(9):11734–11752, September 2018. doi: 10.1021/acssuschemeng.8b01983.